

## Proton Aurora on the Dayside

F. Sigernes<sup>1</sup>, G. Fasel<sup>2</sup>, C.S. Deehr<sup>2</sup>,

R.W. Smith<sup>2</sup>, D.A. Lorentzen<sup>3</sup>, L.T. Wetjen<sup>3</sup> and K. Henriksen<sup>3</sup>

<sup>1</sup>The University Courses on Svalbard, 9170 Longyearbyen, Norway

<sup>2</sup>Geophysical Institute, University of Alaska, Fairbanks, Alaska

<sup>3</sup>The Auroral Observatory, University of Tromsø, 9037 Tromsø, Norway

### Abstract

A simple procedure to evaluate the Balmer excitation rates of  $H_{\alpha}$  and  $H_{\beta}$  to produce the corresponding volume emission rates vs. height, using semi-empirical range relations of protons in air is used. The calculations are carried out with identified ion-energy particle spectra of the dayside aurora obtained by low altitude satellites. It is found that the calculated emission intensities of  $H_{\alpha}$  and  $H_{\beta}$  are observable by ground-based optical devices. Observations of the dayside aurora at Longyearbyen, Svalbard, are discussed in relation to these calculations. Furthermore, when the time between successive proton events on the dayside decrease, the emission ratio of  $H_{\alpha}$  and  $H_{\beta}$  fluctuates indicating a step-like behaviour in the primary initial proton energy.

### Introduction

Around the vicinity of the subsolar point magnetic merging is most likely to occur (Cowley, 1982), merging of interplanetary geomagnetic field lines. Because of the action of the solar wind these field lines are pushed polewards and opening are made for direct entry of solar wind particles to the upper atmosphere. The opening occurs in a region with magnetosheath and magnetospheric particles, and therefore newly opened flux tubes receive such particles. During the merging process the ions are accelerated to about twice the Alfvén velocity. These ions, mainly protons, can travel into the atmosphere and have been identified by low altitude satellite measurements. These measurements have shown step like patterns in the ion energy-time profiles (Smith and Lockwood, 1990; Lockwood and Smith, 1992), which are common cusp precipitation signatures for ions (Lockwood et al., 1993). The newly opened flux tubes are probably the source region of cusp precipitation, and each step and variations in the ion energy-time plot may indicate opening of geomagnetic field lines. Precipitation of electrons into the ionosphere also occurs by the same process, and the electrons interact with atomic oxygen producing both red [OI] 6300 Å and green [OI] 5577 Å emissions through direct and indirect excitation processes.

A unique ground-based signature of the cusp may be obtained if the identified pulsating Balmer emissions on the dayside can be associated with newly opened flux tubes. Protons are the dominant positive charge component of the

solar wind with minor traces of helium and other heavier ions (Henriksen et al., 1978; 1985). The intensity of Balmer emissions in the cleft is normally a few tens of  $R$  and hard to distinguish from interfering  $OH$  and auroral emissions. Therefore studies of the proton aurora require high sensitive ground-based instruments. Proton precipitation causes a widespread weak diffuse aurora due to the ability of the primary proton/hydrogen particles to travel with constant pitch-angle and numerous charge exchanges before they end as thermic particles (Sigernes et al., 1993a), and the efficiency of low-energy protons may be on order of magnitude less than previously predicted by Eather (1967). In this study we provide a simple procedure to evaluate the volume emission height profiles of  $H_\alpha$  and  $H_\beta$ , using measured cusp spectra of protons by the DMSP satellites. The dominating excitation source for these Balmer lines is proton precipitation into the atmosphere. These calculations are then used to estimate a threshold for optical ground-based instruments, detecting signatures due to measured proton precipitation. In this paper we report on the first observations of pulsating proton events in the dayside aurora and they are measured from Longyearbyen, Svalbard. We make no claims to the location of the optical cusp during the events because no simultaneous observations of particle precipitation and imaging auroral measurements were made.

## Calculations and measurements

Calculations are carried out to predict the intensities of the incoming particle spectra as observed by the DMSP satellites crossing the dayside auroral region. The volume emission height profiles of  $H_\alpha$  and  $H_\beta$  are calculated and corresponding ratios are discussed, along with a routine to filter out overlapping emissions in the nearby region of  $H_\alpha$ . The ground truth is obtained from the optical instruments at the observing side, Nordlysstasjonen, Svalbard.

The particle spectra used in this investigation are from the DMSP F7 and F9 satellites crossing the cusp in the southern hemisphere for January 26, 1984. The satellites are in sun-synchronous circular orbits at altitudes of about 800 km. The detector apertures are oriented toward geomagnetic zenith, which means that only field-aligned particles are observed, well within the atmospheric loss cone. These input spectra are chosen, because Newell et al. (1991) identified these particle spectra to correspond to regions in the ionosphere which map back into the magnetosphere as proposed by Vasyliunas (1979). Using the results by Newell et al. (1991), differential ion energy flux spectra of the Cusp<sup>(1)</sup>, the Mantle<sup>(2)</sup> and the Low-latitude boundary layer (LLBL<sup>(3)</sup>) were obtained by fitting Gaussian distributions to the fluxes of the respective regions of interest. The Mantle particle signature has the most intense energy flux (about  $10^6$  ions/cm<sup>2</sup> s sr keV) at 0.3 keV, with the LLBL having a similar maximum, but shifted about 0.4 keV towards higher energies. Both the Mantle<sup>(2)</sup> and the

LLBL(3) particle spectra have relative low intensities compared to the Cusp(1), which is peaked at 0.7 keV with a energy particle flux of about  $10^7$  ions/cm<sup>2</sup> s sr keV.

Since the measured particle flux is highly field-aligned, we assume the complete pitch-angle distribution to be a cosine function, and according to Newell et al., (1991) these data are considered as typical, even if exceptions are easy to find.

Knowing the differential energy particle spectrum above the atmosphere, it is possible to calculate the resulting volume emission rate of  $H_\alpha$  and  $H_\beta$  as a function of height (Sigernes et al., 1993b). In these calculations the main assumptions are that the geomagnetic field is parallel and vertical, and that the pitch-angle of the proton/hydrogen atom is preserved in collisions with

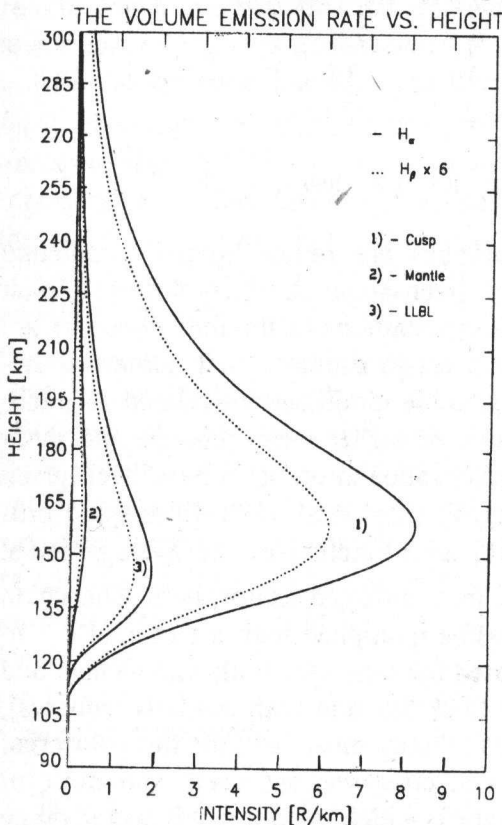


Fig. 1. Calculated volume emission rates of  $H_\alpha$  (solid lines) and  $H_\beta$  (dotted lines) as a function of height. The calculations are based on particle measurements by the DMSP F7 and F9 satellites of the Cusp(1), the Mantle (2) and the Low-latitude boundary layer (LLBL(3)) (Newell et al., 1991). The pitch-angle distribution is assumed to be a cosine function.

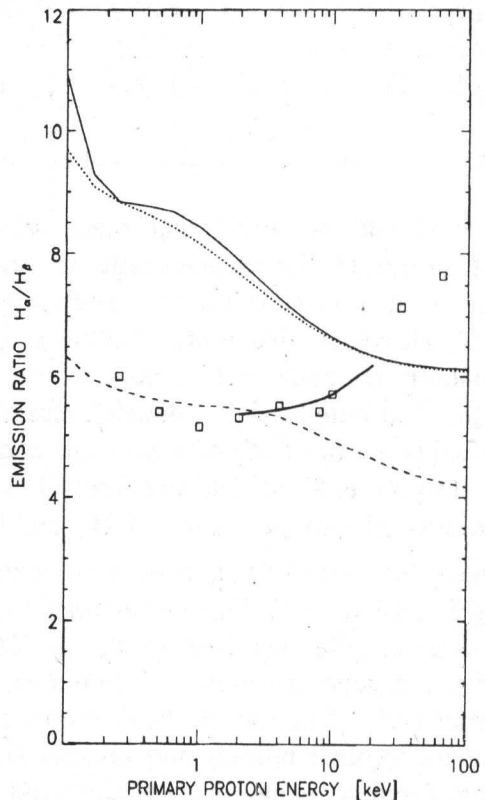


Fig.2. Calculated emission ratios of  $H_\alpha/H_\beta$  as a function of primary energy for an initial monoenergetic particle distribution (solid line) and a Maxwellian distribution (dotted line). Corresponding ratios calculated by Van Zyl et al. (1984) using a Maxwellian distribution is shown (dashed line). Thick line is calculated ratios by Rees (1982) for Maxwellian distributions, while the monoenergetic is plotted with symbols (squares). The pitch-angle for the precipitating particles is zero.

atmospheric constituents before being thermalized. The effective excitation cross sections are from Van Zyl et al. (1980), and the model atmosphere used is MSIS-86 (Hedin, 1987).

Fig. 1 shows the calculated volume emission rate height profiles of  $H_{\alpha}$  (solid lines) and  $H_{\beta}$  (dotted lines) using particle spectra from the DMSP satellites of the Cusp<sup>(1)</sup>, the Mantle<sup>(2)</sup>, and the LLBL<sup>(3)</sup>. Note that the calculated intensities of  $H_{\beta}$  is multiplied by a factor of 6 to be visualized in the same plot as  $H_{\alpha}$ . Table 1 gives the maximum emission altitudes for these profiles, the total height integrated intensities, and the ratios between  $H_{\alpha}$  and  $H_{\beta}$ .

Region	Height of max. Int. [km]	Total Int. $I(H_{\alpha})$ [R]	Total Int. $I(H_{\beta})$ [R]	Ratio $I(H_{\alpha})/I(H_{\beta})$
Cusp(1)	158.0	606.7	76.6	7.9
Mantle(2)	161.0	27.2	3.4	8.0
LLBL(3)	145.0	122.8	16.2	7.6

Table 1: Parameters of calculated volume emission rate vs. height profiles.

It should be noted that these calculations are rather limited, predicting emission ratios for particles only with zero pitch-angle. A totally different result may occur if broader flux and pitch-angle distributions of the initial protons are used. However, this approximation gives a rough estimate, and numerical calculations are under way to indicate the possible modifications related to pitch-angle distributed ions. A detailed discussion of earlier measurements and theoretical predictions of corresponding intensity ratios in question have been given by Van Zyl et al. (1984) and Rees (1982). Van Zyl et al. (1984) predicted proton auroral intensity ratios of  $H_{\alpha}$  and  $H_{\beta}$  as a function of the average initial energy for Maxwellian proton showers in a nitrogen atmosphere, shown in Fig. 2 (dashed line). Our calculations must be multiplied with a factor of 0.7 to fit these calculations. Rees (1982) calculated the ratios for both Maxwellian and monoenergetic distributions, plotted as a thick line and with symbols (squares), respectively. The root of the discrepancy in theory must lie in the three different and incomplete models and uncertainties in cross-sections used, and none of these predictions can explain measured ratios, which yield a much wider range from 1.65 to 7 (Eather, 1967, 1969). The models have not considered collisional decay to the  $3s$  state, missing oxygen cross-sections favouring production of  $n = 4$  hydrogen atoms, or observational problems such as spectral contamination and calibration of the weak and large Doppler shifted hydrogen profiles. All these factors have to be handled and reveal the need for future studies.

Influence of airglow  $OH(6, 1)$  and auroral  $N_2 1P$  in the nearby region of  $H_{\alpha}$  makes it hard to measure true intensities. The main problem is to filter out the



contribution from the airglow, because the  $OH$  rotational lines exist within the  $H_\alpha$  Doppler broadened profile. When the electron precipitation is sufficiently energetic  $N_2$  1P bands are produced close to the  $H_\alpha$  emission, and in addition the proton/hydrogen particle has a significant efficiency for producing  $N_2$  1P bands.

In order to get a clean measured  $H_\alpha$  profile at least two calculated rotational lines of  $OH(6, 1)$  outside the region of  $H_\alpha$  has to be fitted to the corresponding measured lines. Fig. 3 shows an example of data averaged over a time period of 4 hours from the wavelength region (6515-6585) Å obtained the 12 January 1992 with the synthetic  $OH(6, 1)$  spectra plotted on top. During this time period the measuring device, one spectrometer, was fixed in geomagnetic zenith, and no auroral activity was obtained. The North-American Nebular is situated far off zenith, which indicates that the resulting narrow profile at 6563 Å plotted in the lower part of Fig. 3 is geocoronal  $H_\alpha$ , and the emission line close to the  $P_1(1)$  line coincide with the ionized nitrogen line ( $3d^3D^0 - 4p^3D$ ). These measurements were made well inside the polar cap during quiet magnetic conditions, and thus we consider the measured narrow  $H_\alpha$  emission to be essentially of geocoronal origin.

Pulsating Balmer emissions are identified by combining observations from meridian scanning photometers and spectrometers. These temporal variations seem to occur in all kinds of dayside proton aurora, but its low intensity has up to nonprevented its identification.

## Concluding remarks

The principal results obtained by calculations and observations may be summarized as follows.

1. Optical ground-based instruments are in principle capable of detecting signatures produced by initial differential ion-energy particle spectra measured by low altitude satellites crossing the Cusp, the Mantle and the LLBL.

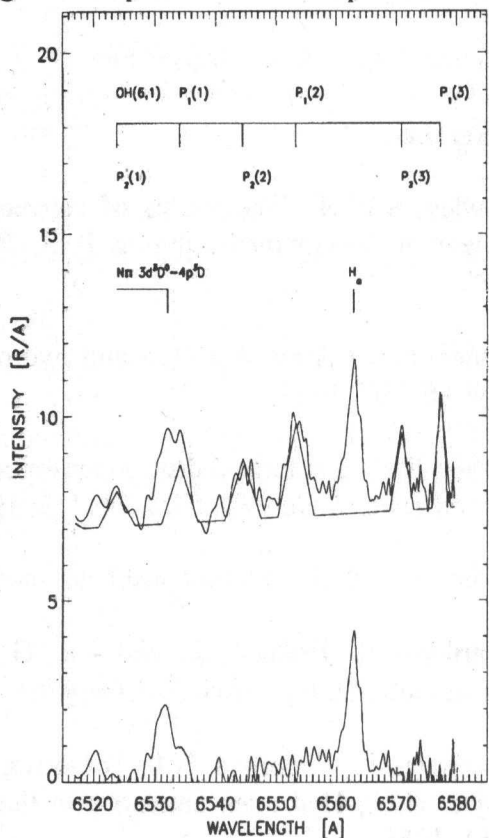


Fig. 3. Calculated synthetic spectra of  $OH(6, 1)$  plotted on top of a measured spectra from Longyearbyen. The spectrometer was scanning the wavelength region (6517-6579) Å, and the result is time averaged over a 4 hr time period. The intensity is given in Rayleigh per Ångström. Each identified emission line is mark at the top of the plot. The bottom part of the plot shows the result of the synthetic  $OH(6, 1)$  filtering, leaving only the geocoronal  $H_\alpha$  and a nitrogen ion line above the noise or background level.

2. Pulsed proton events are observed in the dayside aurora. The narrow width of the measured Doppler shifted  $H_{\alpha}$ -profile indicates that the events are due to low-energy protons. It is also found that when the time elapsed between each individual proton event decrease, the intensity and the corresponding difference in the  $H_{\alpha}/H_{\beta}$ -ratios increase, indicating a step in initial primary energy between events.

3. High spectral resolution ground-based measurements of the total  $H_{\alpha}$  and  $H_{\beta}$  Doppler shifted profiles have to be carried out in order to get true ratios, which in future can be compared to extended model calculations. Sensitivity and temporal resolution of spectrometric observations must also be improved to promote progress.

## References

Cowley, S.W.H., The causes of convection in the earth's magnetosphere: A review of developments during IMS, *Rev. Geophys. Space Phys.*, **20**, 531, 1982.

Eather, R.H., Auroral proton and hydrogen emissions, *Rev. Geophys. Space Phys.*, **5**, 207, 1967.

Eather, R.H., Latitudinal distribution of auroral and airglow emissions: the 'soft' auroral zone, *J. Geophys. Res.* **74**, 153, 1969.

Hedin, A.E., MSIS-86 thermospheric model, *J. Geophys. Res.*, **66**, 4649, 1987.

Henriksen, K., Holback, B., and Witt, G., Variations in the auroral spectrum at the latitude of the polar cleft, *J. Geophys. Res.*, **44**, 401, 1978.

Henriksen, K., Fedorova, N.I., Totunova, G.T., Deehr, C.S., Romick, G.J., and Sivjee, G.G., Hydrogen emissions in the polar cleft, *J. Atm. Terr. Phys.*, **47**, 1051, 1985.

Lockwood, M., Denig, W.F., Farmer, A.D, Dauda, U.N., Cowley, S.W.H., and Luhr, H., Ionospheric signatures of Pulsed Reconnection at the Earth's Magnetopause, *Nature*, **361**, 424, 1993.

Lockwood, M., and Smith, M.F., The variation of Reconnection rate at the Dayside magnetopause and Cusp Ion Precipitation, *J. Geophys. Res.*, **97**, 14841, 1992.

Newell, P.T., Burke, W.J., Meng, C.-I., Sanchez, E.R., and Greenspan, M., Identification and Observation of the Plasma Mantle at Low Altitude, *J. Geophys. Res.*, **96**, 35, 1991.

Rees, M. H., On the interaction of auroral protons with the Earth's atmosphere, *Planet. Space. Sci.*, **30**, 463, 1982.

Smith, M.F., and Lockwood, M., The Pulsating Cusp, *Geophys. Res. Lett.*, **17**, 1069, 1990.

Sigernes, F., Lorentzen, D.A, Deehr, C.S., and Henriksen, K., Calculation of Auroral Balmer volume emission height profiles in the upper atmosphere, accepted by *J. Atm. Terr. Phys.*, May 1993b.

Van Zyl, B. and Neumann, H.,  $H_{\alpha}$  and  $H_{\beta}$  Emission Cross Sections for Low-Energy H and  $H^{+}$  Collisions With  $N_2$  and  $O_2$ , *J. Geophys. Res.* **85**, 6006, 1980.

Van Zyl, B., Gealy, M. W., and Neuman, H., Prediction of Photon Yields for Proton Aurorae in  $N_2$  Atmosphere, *J. Geophys. Res.*, **89**, 1701, 1984.

Vasyliunas, V.M., Interaction between the magnetospheric boundary layers and the ionosphere, Proceedings of Magnetospheric Boundary Layer Conference, *Eur. Space Agency Spec. Publ.*, 148, 1979.